The Coupled-Channel Method for Modelling Quantum Transmission of Composite Systems

S.I. Vinitsky[1,2(✉)], A.A. Gusev[1], O. Chuluunbaatar[1,5], A. Góźdź[3], and V.L. Derbov[4]

[1] Joint Institute for Nuclear Research, Dubna, Russia
vinitsky@theor.jinr.ru
[2] RUDN University (Peoples' Friendship University of Russia), 6 Miklukho-Maklaya Street, Moscow 117198, Russia
[3] Institute of Physics, University of Maria Curie-Sklodowska, Lublin, Poland
[4] Saratov State University, Saratov, Russia
[5] Institue of Mathematics, National University of Mongolia, University Street, Sukhbaatar District, Ulaanbaatar, Mongolia

Abstract. The description of quantum transmission of composite systems of barriers or wells using the coupled-channel method is presented. In this approach the multichannel scattering problem for the Schrödinger equation is reduced to a set of coupled second-order ordinary differential equations with the boundary conditions of the third type and solved using the finite element method. The efficiency of the proposed approach is demonstrated by the example of analyzing metastable states that appear in composite quantum systems tunnelling through barriers and wells and give rise to the quantum transparency and total reflection effects.

Keywords: Coupled-channel method · Quantum tunnelling · Second-order ordinary differential equations · Finite element method software

1 Introduction

Quantum tunnelling of composite systems through barriers is one of the problems most often occurring in nuclear physics, physics of solid state and semiconductor nanostructures. Usually the theory is based on considering the penetration of a structureless particle through barriers within the effective mass approximation [19]. However, the majority of important applications deal with tunnelling of structured objects (clusters), e.g., atomic nuclei through Coulomb barrier, where the effects of structure (multiple particles) manifest themselves in anomalous behaviour of nuclear reaction cross-sections below the Coulomb barrier [20]. Indeed, when the cluster size is comparable with the spatial width of the barrier, the mechanisms arise that enhance the barrier transparency. The effect of quantum barrier transparency depending on the internal structure of the incident particles was revealed for a pair of coupled particles tunnelling through a repulsive barrier [9]. The effect was shown to be due to the barrier resonance formation under the condition that the potential energy of the compound system (cluster + barriers) possesses local minima, thus providing the

V.M. Vishnevskiy et al. (Eds.): DCCN 2016, CCIS 678, pp. 525–537, 2016.
DOI: 10.1007/978-3-319-51917-3_45

appearance of metastable states of the moving cluster [8]. The manifestations and the underlying mechanisms of the effect were extensively studied in multiple quantum phenomena [14–18, 20–23], for example, near-surface quantum diffusion of molecules [10], channelling and tunnelling of ions through multidimensional barriers [2, 5, 11, 22, 24], and sub-barrier tunnelling of light nuclei [12], and the collinear ternary fission [13]. A method and programs for solving the tunnelling of a system of n identical particles coupled by oscillator-type potentials through repulsive barriers has been presented in [1, 3, 4, 6, 7], while their application to study of a transmission of composite systems of both barriers and wells is actual problem in the field.

In present paper we consider the problem of a transmission of composite systems of barriers or wells in the framework of the coupled-channel method basing on the Galerkin-type and Kantorovich methods and discuss conditions of their applicability. By the examples of particles with different coupling potentials, transmission of composite systems as of Gaussian barriers or wells, the transmission coefficients, and the metastable states are analyzed. The energy dependencies of these coefficients demonstrate the phenomena of quantum transparency and total reflection.

The structure of paper is following. In Sect. 2 the coupled-channel method and the multichannel scattering problem are formulated. In Sect. 3 the transmission of clusters comprising several identical particles coupled by oscillator and double-well polynomial potentials are studied separately: tunneling through barrier, transmission above barriers and wells. In Conclusion the results and perspectives are discussed.

2 Problem Statement

2.1 Coupled-Channel Method

Consider the boundary-value problem (BVP) for the equation

$$\left(\hat{H}_f(\mathbf{x}_f;x_s)+\hat{H}_s(x_s)+\check{V}_{fs}(\mathbf{x}_f,x_s)-\mathcal{E}_t\right)\Psi_t(\mathbf{x}_f,x_s)=0 \tag{1}$$

with fast $\mathbf{x}_f$ and slow x_s variables. The operators $\hat{H}_f(\mathbf{x}_f;x_s)$ and $\hat{H}_s(x_s)$ describe the fast and slow subsystem

$$\hat{H}_f(\mathbf{x}_f;x_s) = -\frac{1}{g_{1f}(\mathbf{x}_f)}\frac{\partial}{\partial \mathbf{x}_f}g_{2f}(\mathbf{x}_f)\frac{\partial}{\partial \mathbf{x}_f}+\check{V}_f(\mathbf{x}_f;x_s), \tag{2}$$

$$\hat{H}_s(x_s) = -\frac{1}{g_{1s}(x_s)}\frac{\partial}{\partial x_s}g_{2s}(x_s)\frac{\partial}{\partial x_s}+\check{V}_s(x_s), \tag{3}$$

$\check{V}_f(\mathbf{x}_f;x_s)$ and $\check{V}_s(x_s)$ are the potentials of the fast and slow subsystem, and $\check{V}_{fs}(\mathbf{x}_f,x_s)$ is the interaction potential. The solution $\Psi_t(\mathbf{x}_f,x_s)$ of the problem (1) with the appropriate boundary conditions is sought in the form of Kantorovich expansion

$$\Psi_t(\mathbf{x}_f, x_s) = \sum_{j=1}^{j_{\max}} B_j(\mathbf{x}_f; x_s)\chi_{jt}(x_s). \tag{4}$$

The trial functions $B_j(\mathbf{x}_f; x_s)$ are chosen to be eigenfunctions of the Hamiltonian $\hat{H}_f(\mathbf{x}_f; x_s)$ with the eigenvalues $\hat{E}_j(x_s)$, parametrically depending on $x_s \in \Omega(x_s)$:

$$\hat{H}_f(\mathbf{x}_f; x_s)B_j(\mathbf{x}_f; x_s) = \hat{E}_j(x_s)B_j(\mathbf{x}_f; x_s). \tag{5}$$

These functions satisfy the orthonormality conditions with the weighting function $g_{1f}(\mathbf{x}_f)$ in the same interval $\mathbf{x}_f \in \Omega_{\mathbf{x}_f}(x_s)$:

$$\int_{\mathbf{x}_f^{\min}(x_s)}^{\mathbf{x}_f^{\max}(x_s)} B_i(\mathbf{x}_f; x_s)B_j(\mathbf{x}_f; x_s)g_{1f}(\mathbf{x}_f)d\mathbf{x}_f = \delta_{ij}. \tag{6}$$

Substitution of (4) into (1) yields a BVP for a set of ODEs with respect to the unknown vector functions $\chi_t(x_s) = (\chi_{1;t}(x_s), ..., \chi_{j_{\max;t}}(x_s))^T$ of the slow subsystem, corresponding to the unknown eigenvalues $2E_t \equiv \mathcal{E}_t$,

$$\begin{aligned}
&\Big(\mathbf{D} + \mathbf{E}(x_s) + \mathbf{W}(x_s) - \mathbf{I}\mathcal{E}_t\Big)\boldsymbol{\chi}_t(x_s) = 0,\\
&\mathbf{D} = -\frac{1}{g_{1s}(x_s)}\mathbf{I}\frac{d}{dx_s}g_{2s}(x_s)\frac{d}{dx_s} + \mathbf{I}\check{V}_s(x_s),\\
&\mathbf{W}(x_s) = \mathbf{V}(x_s) + \frac{g_{2s}(x_s)}{g_{1s}(x_s)}\mathbf{H}(x_s) + \frac{1}{g_{1s}(x_s)}\frac{dg_{2s}(x_s)\mathbf{Q}(x_s)}{dx_s} + \frac{g_{2s}(x_s)}{g_{1s}(x_s)}\mathbf{Q}(x_s)\frac{d}{dx_s}
\end{aligned} \tag{7}$$

with the effective potentials $H_{ij}(x_s)$ and $Q_{ij}(x_s)$ defined as

$$\begin{aligned}
V_{ij}(x_s)&=V_{ji}(x_s)=\int_{\mathbf{x}_f^{\min}(x_s)}^{\mathbf{x}_f^{\max}(x_s)} B_i(\mathbf{x}_f; x_s)\check{V}_{fs}(\mathbf{x}_f, x_s)B_j(\mathbf{x}_f; x_s)g_{1f}(\mathbf{x}_f)d\mathbf{x}_f,\\
H_{ij}(x_s)&=H_{ji}(x_s)=\int_{\mathbf{x}_f^{\min}(x_s)}^{\mathbf{x}_f^{\max}(x_s)} \frac{\partial B_i(\mathbf{x}_f; x_s)}{\partial x_s}\frac{\partial B_j(\mathbf{x}_f; x_s)}{\partial x_s}g_{1f}(\mathbf{x}_f)d\mathbf{x}_f,\\
Q_{ij}(x_s)&=-Q_{ji}(x_s)=-\int_{\mathbf{x}_f^{\min}(x_s)}^{\mathbf{x}_f^{\max}(x_s)} B_i(\mathbf{x}_f; x_s)\frac{\partial B_j(\mathbf{x}_f; x_s)}{\partial x_s}g_{1f}(\mathbf{x}_f)d\mathbf{x}_f.
\end{aligned} \tag{8}$$

If the potential of the fast subsystem $\check{V}_f(\mathbf{x}_f; x_s)$ is independent of the slow variable, then the expansion is referred to as Galerkin-type expansion. Its advantage is that the eigenvalue problem (5) should be solved only once. However, if the position of the potential well and, therefore, the localization of eigenfunctions changes, the convergence of Galerkin-type expansions becomes very slow [5]. The example of the effective potentials of double-well potential (from Fig. 1) for Galerkin-type and Kantorovich expansions are shown in Fig. 2. In considered case the Galerkin method is a more appropriate because effective potentials have a smooth behavior, while in Kantorovich method effective potentials have a sharp behavior with a large magnitude due to series of quasicrossing of the potential curves.

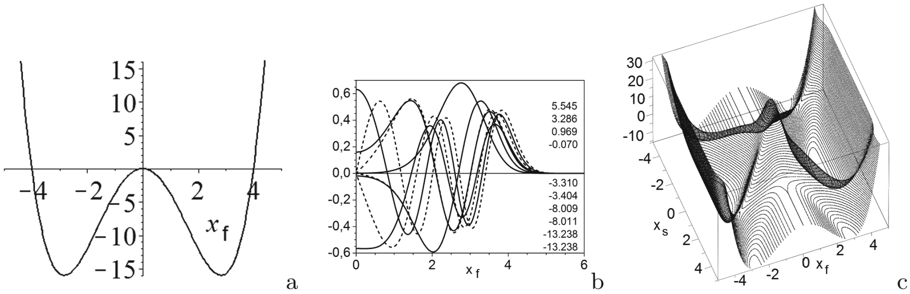

Fig. 1. Double-well interaction potential (a), the first even (solid lines) and odd (dashed lines) eigenfunctions (b), and the corresponding 2D potential $V(x_f) + V^b(x_f; x_s)$ (c).

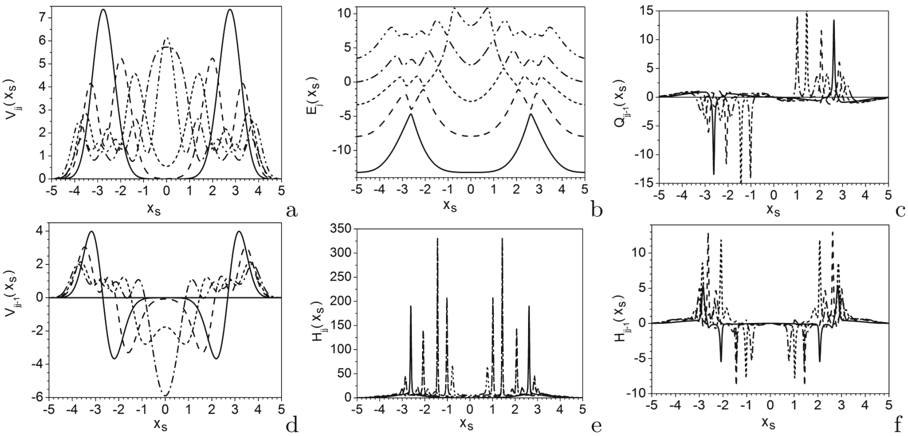

Fig. 2. Even effective potentials for Galerkin-type (a, d) and Kantorovich (b, c, e, f) expansions.

2.2 Scattering Problem

Consider the scattering problem with the homogeneous boundary conditions of the third kind at $x_s = x_s^{\min} \ll 0$ and $x_s = x_s^{\max} \gg 0$:

$$\left.\frac{d\Phi(x_s)}{dx_s}\right|_{x_s = x_s^{\min}} = \mathcal{R}(x_s^{\min})\Phi(x_s^{\min}), \quad \left.\frac{d\Phi(x_s)}{dx_s}\right|_{x_s = x_s^{\max}} = \mathcal{R}(x_s^{\max})\Phi(x_s^{\max}), \quad (9)$$

where $\mathcal{R}(x_s)$ is an unknown $N \times N$ matrix function, $\Phi(x_s) = \{\chi^{(j)}(x_s)\}_{j=1}^{N_o}$ is the desired $N \times N_o$ matrix solution and N_o is the number of open channels, $N_o = \max_{2E \geq \epsilon_j} j \leq N$.

The matrix solution $\Phi_v(x_s) = \Phi(x_s)$, describing the incidence of the particle and its scattering, with the asymptotic form "incident wave + outgoing waves" (see Fig. 4a) is written as

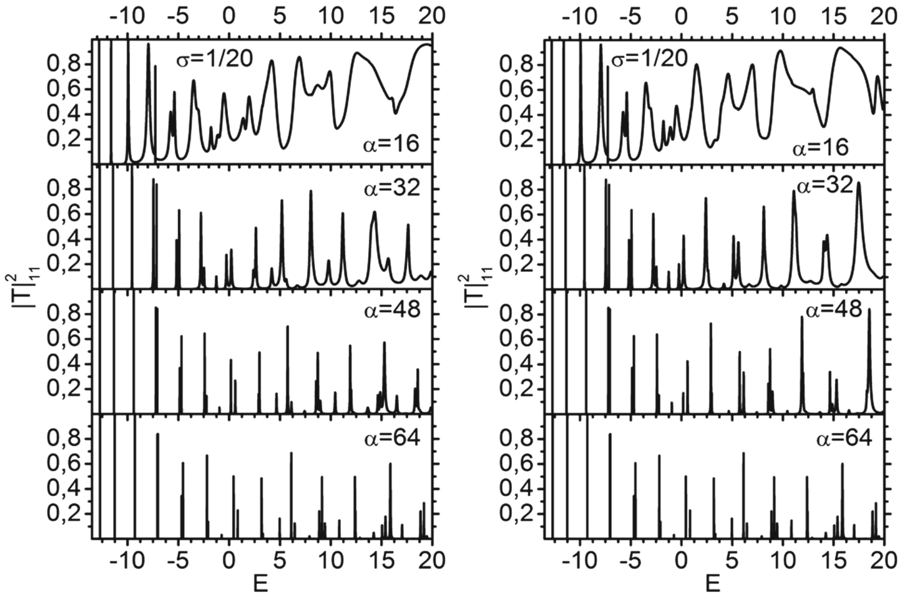

Fig. 3. The total probability of penetration through repulsive Gaussian potential barriers $|\mathbf{T}|^2_{11}$ versus the energy E with the ground and excited initial states.

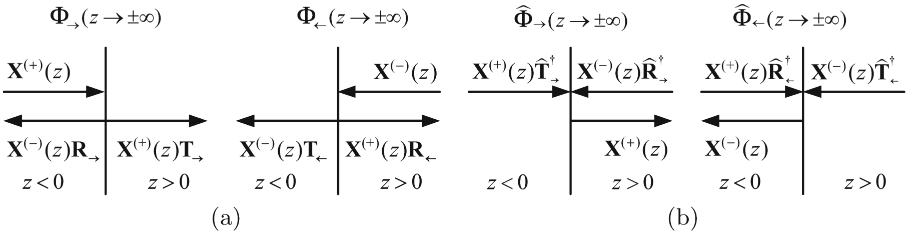

Fig. 4. Schematic diagrams of the wave functions $\Phi_v(z)$ at $z \equiv x_s$ having the asymptotic form: (a) "incident wave + outgoing waves", (b) "incident waves + ingoing wave".

$$\Phi_v(x_s \to \pm\infty) = \begin{cases} \begin{cases} \mathbf{X}^{(+)}(x_s)\mathbf{T}_v, & x_s > 0, \\ \mathbf{X}^{(+)}(x_s) + \mathbf{X}^{(-)}(x_s)\mathbf{R}_v, & x_s < 0, \end{cases} & v = \rightarrow, \\ \begin{cases} \mathbf{X}^{(-)}(x_s) + \mathbf{X}^{(+)}(x_s)\mathbf{R}_v, & x_s > 0, \\ \mathbf{X}^{(-)}(x_s)\mathbf{T}_v, & x_s < 0, \end{cases} & v = \leftarrow, \end{cases} \tag{10}$$

where $\mathbf{R}_v$ and $\mathbf{T}_v$ are the reflection and transmission $N_o \times N_o$ matrices, $v = \rightarrow$ and $v = \leftarrow$ denote the initial direction of the particle motion along the x_s axis. The leading term of the asymptotic rectangular matrix functions $\mathbf{X}^{(\pm)}(x_s)$ has the form [5]

$$X^{(\pm)}_{ij}(x_s) \to p_j^{-1/2} \exp\left(\pm\imath\left(p_j x_s - \frac{Z_j}{p_j}\ln(2p_j|x_s|)\right)\right)\delta_{ij}, \tag{11}$$

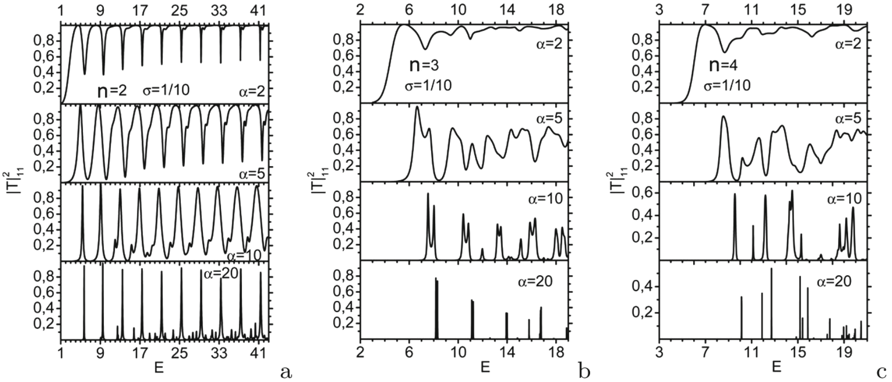

Fig. 5. The total transmission probability $|\mathbf{T}|^2_{11}$ versus the energy E (in oscillator units). Two (a), three (b) and four (c) identical particles, coupled by the oscillator potential, penetrate through the repulsive Gaussian barrier with $\sigma = 0.1$ and $\alpha = 2, 5, 10, 20$. The system is initially in the ground state.

$$p_j = \sqrt{2E - \epsilon_j} \quad i = 1, \ldots, N, \quad j = 1, \ldots, N_o,$$

where $Z_j = Z_j^+$ at $x_s > 0$ and $Z_j = Z_j^-$ at $x_s < 0$. The matrix solution $\Phi_v(x_s, E)$ is normalized by the condition

$$\int_{-\infty}^{\infty} \Phi^\dagger_{v'}(x_s, E')\Phi_v(x_s, E)dx_s = 2\pi\delta(E' - E)\delta_{v'v}\mathbf{I}_{oo}, \tag{12}$$

where $\mathbf{I}_{oo}$ is the unit $N_o \times N_o$ matrix.

Let us rewrite Eq. (10) in the matrix form at $x_s^+ \to +\infty$ and $x_s^- \to -\infty$ as

$$\begin{pmatrix} \Phi_\to(x_s^+) & \Phi_\leftarrow(x_s^+) \\ \Phi_\to(x_s^-) & \Phi_\leftarrow(x_s^-) \end{pmatrix} = \begin{pmatrix} \mathbf{0} & \mathbf{X}^{(-)}(x_s^+) \\ \mathbf{X}^{(+)}(x_s^-) & \mathbf{0} \end{pmatrix} + \begin{pmatrix} \mathbf{0} & \mathbf{X}^{(+)}(x_s^+) \\ \mathbf{X}^{(-)}(x_s^-) & \mathbf{0} \end{pmatrix} \mathbf{S}, \tag{13}$$

where the unitary and symmetric scattering matrix $\mathbf{S}$

$$\mathbf{S} = \begin{pmatrix} \mathbf{R}_\to & \mathbf{T}_\leftarrow \\ \mathbf{T}_\to & \mathbf{R}_\leftarrow \end{pmatrix}, \qquad \mathbf{S}^\dagger\mathbf{S} = \mathbf{S}\mathbf{S}^\dagger = \mathbf{I} \tag{14}$$

is composed of the reflection and transmission matrices. Detailed calculation of the matrix solution $\Phi_v(x_s)$ is presented in Reference [4].

3 Transmission of Clusters Comprised by Several Identical Particles

Consider a cluster of two or three identical particles with the masses m coupled via the pair potentials $\tilde{U}^{pair}(x_{tt'})$, $x_{tt'} = x_t - x_{t'}$ propagated the barrier or well $\tilde{V}(x_t)$. The wave function of this system satisfies the Schrödinger equation

$$\left[-\sum_{t=1}^{n} \frac{\partial^2}{\partial x_t^2} + \sum_{t,t'=1;t<t'}^{n} \frac{(x_{tt'})^2}{n} + \sum_{t,t'=1;t<t'}^{n} U^{pair}(x_{tt'}) + \sum_{t=1}^{n} V(x_t) - E \right] \Psi(\mathbf{x}) = 0. \tag{15}$$

Here E is the total energy of n particles, $V(x_t)=\tilde{V}(x_t x_{osc})/E_{osc}$ is the barrier or the well potential, $V^{hosc}(x_{tt'})=\tilde{V}^{hosc}(x_{tt'}x_{osc})/E_{osc}=\frac{1}{n}(x_{tt'})^2$ is the harmonic oscillator potential, $V^{pair}(x_{tt'})=\tilde{V}^{pair}(x_{tt'}x_{osc})/E_{osc}$ and $U^{pair}(x_{tt'})=V^{pair}(x_{tt'})-V^{hosc}(x_{tt'})$ is the effective pair potential given in the oscillator units. In the symmetric coordinates [4,6]:

$$\xi_0=\frac{1}{\sqrt{n}}\sum_{t=1}^{n}x_t,\quad \xi_{t'}=\frac{1}{\sqrt{n}}\left(x_1+\sum_{t=2}^{n}a_0x_t+\sqrt{n}x_{t'+1}\right),\quad t'=1,...,n-1,\quad (16)$$

where $a_0=1/(1-\sqrt{n})<0$, $a_1=a_0+\sqrt{n}$, Eq. (15) takes the form

$$\left[-\frac{\partial^2}{\partial\xi_0^2}+\sum_{i=1}^{n-1}\left(-\frac{\partial^2}{\partial\xi_i^2}+(\xi_i)^2\right)+U(\xi_0,...,\xi_{n-1})-E\right]\Psi(\xi_0,...,\xi_{n-1})=0,$$

$$U(\xi_0,...,\xi_{n-1})=\sum_{i,j=1;i<j}^{n}U^{pair}(x_{ij}(\xi_1,...,\xi_{n-1}))+\sum_{i=1}^{n}V(x_i(\xi_0,...,\xi_{n-1})).\quad (17)$$

Here $x_s=\xi_0$ in the center-of-mass variable and $\mathbf{x}_f=\{\xi_1,...,\xi_{n-1}\}$ is the set of relative variables, such that at $n=2$ they correspond to the Jacobi coordinates (Fig. 8).

Double-Well Interaction Potential. Now consider a pair of particles, coupled by the double-well interaction potential $V(x_f)=x_f^4/4-4x_f^2$ (see Fig. 1a) tunnelling through the repulsive Gaussian barriers $V_i(x_i)=\alpha\exp(-x_i^2/2\sigma)$ with $\alpha=16,32,48,64$, $\sigma=1/20$. In this case Eq. (15) takes the form

$$\left(-\frac{\partial^2}{\partial x_s^2}-\frac{\partial^2}{\partial x_f^2}+V(x_f)+V^b(x_f;x_s)-2E\right)\Psi(x_f,x_s)=0,\qquad (18)$$

where $V^b(x_f;x_s)=V_1(x_1)+V_2(x_2)$.

The first even and odd eigenfunctions are presented in Fig. 1b. The typical behaviour of symmetric double-well potential eigenfunctions is seen, namely, for $E<0$ there are pairs of even and odd eigenfunctions localized in the potential wells, with closely spaced energy levels. For $E>0$ the energy levels of even and odd states alternate. The corresponding 2D potential is demonstrated in Fig. 1c.

In this case we have two possibilities to construct the fast, slow, and interaction potential, corresponding either to the Galerkin-type expansion

$$\check{V}_f(x_f;x_s)=V(x_f),\quad \check{V}_s(x_s)=0,\quad \check{V}_{fs}(x_f,x_s)=V^b(x_f;x_s),$$

or the Kantorovich expansion

$$\check{V}_f(x_f;x_s)=V(x_f)+V^b(x_f;x_s),\quad \check{V}_s(x_s)=0,\quad \check{V}_{fs}(x_f,x_s)=0.$$

The effective potentials (8) are presented in Fig. 2. It is seen that the non-diagonal matrix elements in the case of Kantorovich expansion are small as compared to the case of Galerkin-type expansion, except some areas, corresponding to quasi-crossing of the energy levels in the problem (5) (see Fig. 2b).

Figure 3 shows the energy dependence of the total transmission probability $|\mathbf{T}|^2_{ii} = \sum_{j=1}^{N_o} |T_{ji}(E)|^2$. This is the probability of a transition from a chosen state i into any of N_o states, found by solving the boundary-value problem in the Galerkin form. The behaviour of the probability versus the energy is non-monotonic, and the observed resonances are manifestations of the quantum transparency effect. This effect is caused by the existence of barrier metastable states, embedded in the continuum.

Parabolic Interaction Potential. Two, three or four identical particles (n=2,3,4) are coupled by the harmonic oscillator potential $V(x_t - x_{t'}) = (x_t - x_{t'})^2$, $t', t = 1, ..., n$ and the Gaussian barrier ($\alpha > 0$) or well ($\alpha < 0$): $V(x_t) = \alpha/(\sqrt{2\pi}\sigma)\exp(-x_t^2/\sigma^2)$.

Figure 5 shows the energy dependence of the total transmission probability $|\mathbf{T}|^2_{ii} = \sum_{j=1}^{N_o} |T_{ji}(E)|^2$. This is the probability of a transition from the ground state i to any of N_o eigenstates of the BVP in the Galerkin form solved using the program KANTBP [1,3]. The dependence of the probability upon the energy is non-monotonic, and the observed resonance peaks are manifestations of the quantum transparency effect. The multiplet structure of the peaks for symmetric and antisymmetric states is similar. Due to the symmetry of the potential in the case of two identical particles, the position of the maxima for symmetric and antisymmetric states coincide. In the case of three particles peak positions for symmetric and antisymmetric states are different, but due to the symmetry with respect to the plane $\xi_0 = 0$, explain the presence of doublets.

Figure 6 shows the profiles of $|\Psi|^2 \equiv |\Psi^{(-)}_{Em\to}|^2$ with $\alpha = 20$, $\sigma = 1/10$ at the resonance energies of the first three maxima and the second maximum and the first minimum of the transmission coefficient, illustrating the resonance transmission. It is seen that in the case of resonance transmission the energy is transferred from the centre-of-mass degree of freedom, described by the coordinate ξ_0, to the internal (transverse) one, described by ξ_1 i.e., the transverse oscillator undergoes a transition from the ground state to the excited state. On the contrary, in the case of total reflection the energy transfer is extremely small, and the transverse oscillator returns to infinity in the initial state. In Fig. 7 the first three metastable states are presented. The wave function amplitudes for these states are seen to differ from the amplitudes of the states, corresponding to the first three maxima in the vicinity of wells.

Figure 9 shows the profiles of probability density $|\Psi(\xi_0, \xi_1)|^2$ for the symmetric states of $A = 2$ particles transmitting above Gaussian barrier $\alpha = 2$, $\sigma = 1/10$, revealing total reflection at resonance energies. In Table 1 the values of energies $E^M_m = \Re E^M_m + \imath \Im E^M_m$ of corresponding metastable states for a transmission of $A = 2$ particles above the Gaussian barrier $\alpha = 2$, $\sigma = 1/10$ are presented. One can see that the series of resonances in the transmission $|\mathbf{T}|^2_{11}$ from the ground state 1 are induced by metastable states from second, third, fourth and seventh closed channels, respectively from left to right panels.

In Fig. 10 the total transmission probability $|\mathbf{T}|^2_{11}$ versus the energy E (in oscillator units) for systems of the $A = 2, 3, 4$ particles, coupled by the oscillator potential, propagating above the Gaussian well with $\sigma = 0.1$ and $\alpha = -1, -2$

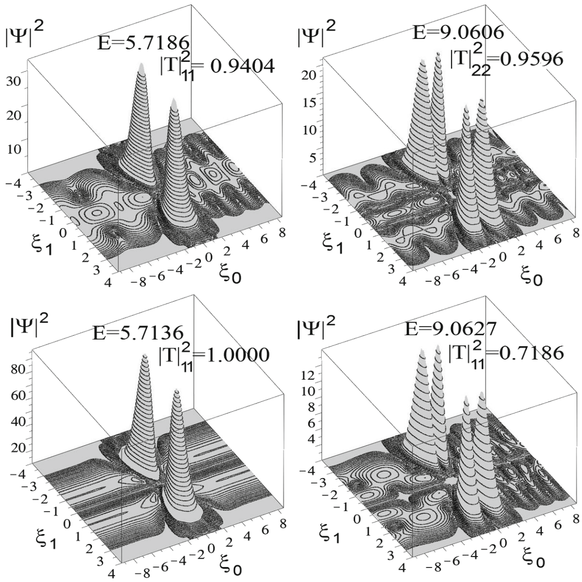

Fig. 6. Profiles of probability densities $|\Psi(\xi_0, \xi_1)|^2$ for symmetric (top panel) and anti-symmetric (bottom panel) states of two particles, revealing resonance transmission and total reflection at resonance energies, shown in Fig. 5.

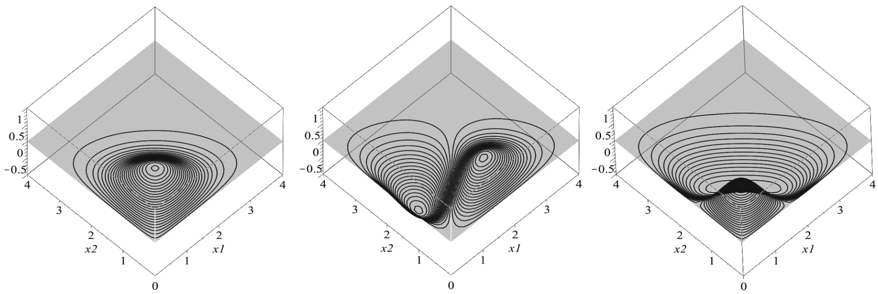

Fig. 7. The first three metastable states corresponding to $E_i^D = 5.76,\ 9.12,\ 9.53$.

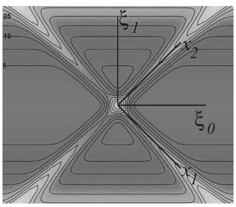

E_i^S	$\vert\mathbf{T}\vert^2_{11}$	$\vert\mathbf{T}\vert^2_{33}$	E_m^M
5.8228	0.3794		
9.6479	0.3779		9.614−ı0.217
13.5548	0.4765		13.505−ı0.144
13.9648		0.8536	14.018−ı0.286
17.4512	0.4874		17.445−ı0.103

Fig. 8. The 2D potential for propagation of two particles ($n = 2$) above the Gaussian barrier $\alpha = 2$, $\sigma = 1/10$ and the values of energies $E_m^M = \Re E_m^M + \imath \Im E_m^M$ of metastable states corresponding to the peaks of $|\mathbf{T}|^2_{11}$ shown in Fig. 5a.

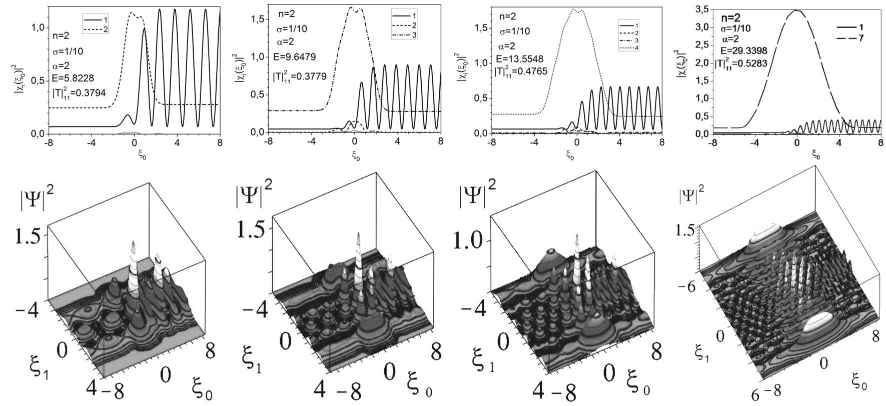

Fig. 9. Profiles of probability densities $|\Psi(\xi_0, \xi_1)|^2$ for symmetric states of two particles transmitted above the Gaussian barrier $\alpha = 2$, $\sigma = 1/10$, revealing resonance transmission and total reflection at resonance energies.

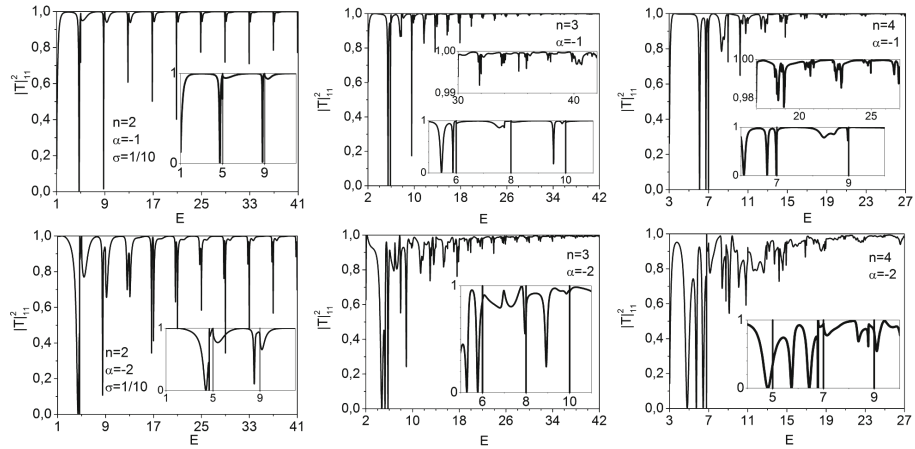

Fig. 10. The total transmission probability $|\mathbf{T}|^2_{11}$ versus the energy E (in oscillator units). The cluster of $n = 2, 3, 4$ particles, coupled by the oscillator potential, propagates above the Gaussian well with $\sigma = 0.1$ and $\alpha = -1, -2$. The system is initially in the ground state. The vertical lines on the epures denote the threshold energies.

are presented. In Table 1 the values of energies $E_m^M = \Re E_m^M + \imath \Im E_m^M$ of the corresponding metastable states for the transmission of $A = 2$, 3 and 4 particles above the Gaussian well $\alpha = -2$, $\sigma = 1/10$ are shown. The energies $E_m^B < E_1^{th}$ of bound states below first threshold E_1^{th} shown in last row. One can see that the resonance structure becomes enriched with increasing the number of transmitted particles. So, in the case of $A = 2$ we see double-resonance structures, similar to the double-well case. In the case of $A = 3$ and 4 the double structure can appear with increasing the depth of wells $|\alpha|$. Figure 11 presents the profiles of

Table 1. The values of energies $E_m^M = \Re E_m^M + \imath \Im E_m^M$ of metastable states for a transmission of a cluster of $A = 2$, 3 and 4 particles above the Gaussian well $\alpha = -2$, $\sigma = 1/10$ shown in Figs. 10 and 11. The energies $E_m^B < E_1^{th}$ of bound states below the first threshold E_1^{th} are shown in last row.

E_i^{th}	$E_m^M(A=2)$	E_i^{th}	$E_m^M(A=3)$	E_i^{th}	$E_m^M(A=4)$
1	4.4348−$\imath$0.2572	2	5.3307−$\imath$0.0620	3	5.7747−$\imath$0.0742
	4.6764−$\imath$0.0058		5.7911−$\imath$0.0621		6.4441−$\imath$0.1050
5	8.5158−$\imath$0.0506	6	6.9922−$\imath$0.0751		6.7934−$\imath$0.0033
	8.7675−$\imath$0.1261		7.9457−$\imath$0.0565	7	8.3668−$\imath$0.0651
9	12.6009−$\imath$0.1215	8	8.9601−$\imath$0.0588		8.7797−$\imath$0.0080
	12.7330−$\imath$0.0142		9.4950−$\imath$0.2251	9	9.4050−$\imath$0.1995
13	16.6841−$\imath$0.0364		9.8617−$\imath$0.0852		9.9926−$\imath$0.1225
	16.7050−$\imath$0.0914	10	11.4173−$\imath$0.1678		10.0755−$\imath$0.0676
Bound states: −0.3588		{−0.2605, 1.5082}		{−0.1938, 1.7084 2.7046}	

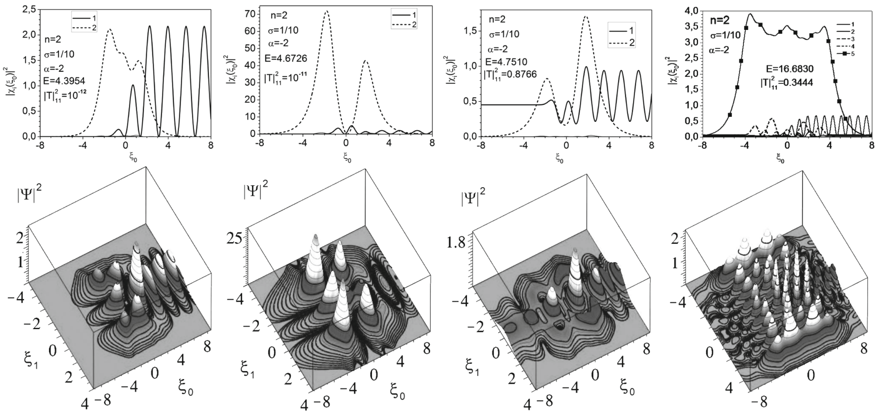

Fig. 11. Profiles of probability density $|\Psi(\xi_0, \xi_1)|^2$ for symmetric states of two particles transmitted above the Gaussian well $\alpha = 2$, $\sigma = 1/10$, revealing total reflection and resonance transmission at the resonance energies.

probability density $|\Psi(\xi_0, \xi_1)|^2$ for the symmetric states of two particles transmitted above the Gaussian well $\alpha = 2$, $\sigma = 1/10$, revealing the resonance transmission and total reflection at resonance energies. One can see that the series of resonances in the transmission $|\mathbf{T}|_{11}^2$ from the ground state 1 are induced by Feshbach metastable states from second and the fifth closed channels, respectively, from left to right panels. In contrast to the case of barrier in the vicinity of the well resonance, we see both the resonance reflection and the transmission (see two middle panels in Fig. 11).

4 Conclusion

We considered the application of the coupled-channel methods to the problem of quantum tunnelling of a cluster of particles coupled by the oscillator-type interactions, through Gaussian potential barriers and above wells. The initial boundary problem is reduced to that for a set ordinary differential equations of the second order. By a few examples we demonstrate the efficiency of the proposed approach for the cluster tunnelling problem and the capability of the method to provide correct description of the cluster tunnelling specific features, including the quantum transparency and total reflection phenomena induced by the shape and Feshbach metastable states. The Kantorovich method finds a more general application in solving multichannel scattering problems with long-range interactions [5,11] and the break-up processes in few-body systems in hyperspherical adiabatic representation [25]. An important advantage of the approach is the possibility of efficient use of symbolic-numeric software packages that considerably simplify the calculations as compared to direct numerical approaches.

The work was supported by the Russian Foundation for Basic Research (grant 14-01-00420) the Bogoliubov-Infeld JINR program, and was funded within the Agreement N 02.03.21.0008 dated 24.04.2016 between the Ministry of Education and Science of the Russian Federation and RUDN University.

References

1. Gusev, A.A., Chuluunbaatar, O., Vinitsky, S.I., Abrashkevich, A.G.: KANTBP 3.0: new version of a program for computing energy levels, reflection and transmission matrices, and corresponding wave functions in the coupled-channel adiabatic approach. Comput. Phys. Commun. **185**, 3341–3343 (2014)
2. Gusev, A.A., Hai, L.L.: Algorithm for solving the two-dimensional boundary value problem for model of quantum tunneling of a diatomic molecule through repulsive barriers. Bull. Peoples' Friendsh. Univ. Russia. Ser. "Math. Inf. Sci. Phys." **1**, 15–36 (2015)
3. Gusev, A.A., Hai, L.L., Chuluunbaatar, O., Vinitsky, S.I.: Programm KANTBP 4M for solving boundary-value problems for systems of ordinary differential equations of the second order (2015). http://wwwinfo.jinr.ru/programs/jinrlib/kantbp4m
4. Gusev, A.A., Vinitsky, S.I., Chuluunbaatar, O., Derbov, V.L., Góźdź, A., Krassovitskiy, P.M.: Metastable states of a composite system tunneling through repulsive barriers. Theor. Math. Phys. **186**, 21–40 (2016)
5. Gusev, A.A., Vinitsky, S.I., Chuluunbaatar, O., Gerdt, V.P., Rostovtsev, V.A.: Symbolic-numerical algorithms to solve the quantum tunneling problem for a coupled pair of ions. In: Gerdt, V.P., Koepf, W., Mayr, E.W., Vorozhtsov, E.V. (eds.) CASC 2011. LNCS, vol. 6885, pp. 175–191. Springer, Heidelberg (2011). doi:10.1007/978-3-642-23568-9_14
6. Gusev, A., Vinitsky, S., Chuluunbaatar, O., Rostovtsev, V., Hai, L., Derbov, V., Góźdź, A., Klimov, E.: Symbolic-numerical algorithm for generating cluster eigenfunctions: identical particles with pair oscillator interactions. In: Gerdt, V.P., Koepf, W., Mayr, E.W., Vorozhtsov, E.V. (eds.) CASC 2013. LNCS, vol. 8136, pp. 155–168. Springer, Heidelberg (2013). doi:10.1007/978-3-319-02297-0_14

7. Vinitsky, S., Gusev, A., Chuluunbaatar, O., Rostovtsev, V., Hai, L., Derbov, V., Krassovitskiy, P.: Symbolic-numerical algorithm for generating cluster eigenfunctions: tunneling of clusters through repulsive barriers. In: Gerdt, V.P., Koepf, W., Mayr, E.W., Vorozhtsov, E.V. (eds.) CASC 2013. LNCS, vol. 8136, pp. 427–442. Springer, Heidelberg (2013). doi:10.1007/978-3-319-02297-0_35
8. Pen'kov, F.M.: Quantum transmittance of barriers for composite particles. J. Exp. Theor. Phys. **91**, 698–705 (2000)
9. Pen'kov, F.M.: Metastable states of a coupled pair on a repulsive barrier. Phys. Rev. A **62**, 044701-1-4 (2000)
10. Pijper, E., Fasolino, A.: Quantum surface diffusion of vibrationally excited molecular dimers. J. Chem. Phys. **126**, 014708-1-10 (2007)
11. Chuluunbaatar, O., Gusev, A.A., Derbov, V.L., Krassovitskiy, P.M., Vinitsky, S.I.: Channeling problem for charged particles produced by confining environment. Phys. Atom. Nucl. **72**, 768–778 (2009)
12. Shotter, A.C., Shotter, M.D.: Quantum mechanical tunneling of composite particle systems: linkage to sub-barrier nuclear reactions. Phys. Rev. C **83**, 054621 (2011)
13. Tashkhodjaev, R.B., Muminov, A.I., Nasirov, A.K., von Oertzen, W., Yongseok, O.: Theoretical study of the almost sequential mechanism of true ternary fission. Phys. Rev. C **91**, 054612 (2015)
14. Gusev, A.A., Vinitsky, S.I., Chuluunbaatar, O., Hai, L.L., Derbov, V.L., Gozdz, A., Krassovitskiy, P.M.: Resonant tunneling of a few-body cluster through repulsive barriers. Phys. At. Nucl. **77**, 389–413 (2014)
15. Sato, T., Kayanuma, Y.: Quantum inelasticity in reflection of a composite particle. Europhys. Lett. **60**, 331–336 (2002)
16. Bertulani, C.A., Flambaum, V.V., Zelevinsky, V.G.: Tunneling of a composite particle: effects of intrinsic structure. J. Phys. G: Nucl. Part. Phys. **34**, 2289–2295 (2007)
17. Flambaum, V.V., Zelevinsky, V.G.: Quantum tunnelling of a complex system: effects of a finite size and intrinsic structure. J. Phys. G: Nucl. Part. Phys. **31**, 355–360 (2005)
18. Bertulani, C.A.: Tunneling of atoms, nuclei and molecules. Few-Body Syst. **56**, 727–736 (2015)
19. Esaki, L.: Long journey into tunneling. Rev. Mod. Phys. **46**, 237–244 (1973)
20. Lemasson, A., et al.: Modern rutherford experiment: tunneling of the most neutron-rich nucleus. Phys. Rev. Lett. **103**, 232701 (2009)
21. Lugovskoy, A.V., Bray, I.: Pseudostate description of diatomic-molecule scattering from a hard-wall potential. Phys. Rev. A **87**, 012904 (2013)
22. Bulatov, V.L., Kornilovitch, P.E.: Anomalous tunneling of bound pairs in crystal lattices. Europhys. Lett. **71**, 352–358 (2005)
23. Muradyan, G., Hakobyan, H., Muradyan, A.Z.: Tunneling dynamics of a two-atom system. J. Phys: Conf. Ser. **672**, 012013 (2016)
24. Bondar, D.I., Liu, W.-K., Ivanov, M.Y.: Enhancement and suppression of tunneling by controlling symmetries of a potential barrier. Phys. Rev. A **82**, 052112 (2010)
25. Chuluunbaatar, O., Gusev, A.A., Derbov, V.L., Kaschiev, M.S., Melnikov, L.A., Serov, V.V., Vinitsky, S.I.: Calculation of a hydrogen atom photoionization in a strong magnetic field by using the angular oblate spheroidal functions. J. Phys. A **40**, 11485–11524 (2007)